Separation Science and Technology
Publication details, including instructions for authors and subscription information:
http://www.informaworld.com/smpp/title~content=t713708471

Electrical Aspects of Adsorbing Colloid Flotation. XI. Surfactant Adsorption Isotherms, Particle Displacement, and Differential Capacitance

Judy E. Kiefer[a]; David Wilson[a]
[a] DEPARTMENT OF CHEMISTRY, VANDERBILT UNIVERSITY, NASHVILLE, TENNESSEE

To cite this Article Kiefer, Judy E. and Wilson, David(1980) 'Electrical Aspects of Adsorbing Colloid Flotation. XI. Surfactant Adsorption Isotherms, Particle Displacement, and Differential Capacitance', Separation Science and Technology, 15: 1, 57 — 74
To link to this Article: DOI: 10.1080/01496398008060253
URL: http://dx.doi.org/10.1080/01496398008060253

SEPARATION SCIENCE AND TECHNOLOGY, 15(1), pp. 57–74, 1980

Electrical Aspects of Adsorbing Colloid Flotation. XI. Surfactant Adsorption Isotherms, Particle Displacement, and Differential Capacitance

JUDY E. KIEFER and DAVID WILSON*

DEPARTMENT OF CHEMISTRY
VANDERBILT UNIVERSITY
NASHVILLE, TENNESSEE 37235

Abstract

Statistical mechanics is used to calculate adsorption isotherms of ionic surfactants on charged solid–water interfaces. The effects of coulombic repulsions between the ionic heads of the surfactant species are taken into account, as are the van der Waals attractions of their hydrocarbon tails. A "squeeze-out" mechanism, by means of which viscous drag forces acting tangentially to the surface of a rising bubble may detach floc particles from it, is examined. A nonideal Poisson-Boltzmann equation is used to calculate the differential capacitance of the electric double layer at an interface.

INTRODUCTION

Foam floatation methods have been used for recovery of trace elements for analysis and for the treatment of simulated and actual industrial wastewaters; a number of comprehensive reviews cover the area (*1–4*). Precipitate and adsorbing colloid flotation techniques have a major advantage over other foam separations in that one does not require stoichiometric quantities (or more) of the collector surfactant; this markedly improves the economics of the process. We here continue our exploration of the theory of the adsorption of floc particles at the air–water interface (*5–12*).

We first examine the adsorption of surfactant onto floc particles to form a hemimicelle, thus rendering the particles hydrophobic and permitting bubble attachment to occur. This model, first used by Gaudin and

*To whom correspondence should be addressed.

Fuerstenau (*13*), has been used extensively by Fuerstenau, Somasundaran, Healy, and others in connection with ore flotation (*14–20*), and has been very useful. We gave a statistical mechanical analysis of the model (*7*), employing a method described by Fowler and Guggenheim (*21*); we subsequently extended the approach to include competitive adsorption of a surfactant and a nonsurfactant species (*8*). In our previous work, however, we did not take very precise account of the coulombic repulsions of the surfactant ionic heads in calculating the interaction energy between adjacent surfactant ions. We here correct that deficiency.

As a general rule, the random thermal forces are very much smaller than the viscous drag forces tending to detach floc particles from bubbles in particle flotation (*7*, *8*). We here explore a "squeeze-out" mechanism by means of which viscous drag forces acting tangentially to the bubble surface may detach floc particles from the bubble. This model was suggested by the results of a rather detailed computation of the viscous drag forces on a particle bound to a rising bubble (*22*).

In the calculations of electric potentials in the vicinity of interfaces, we have generally used a Poisson-Boltzmann equation which takes into account the finite volumes of the ions (*23*). We use this equation to calculate the differential capacitance of the double layer in the vicinity of the interface.

ADSORPTION ISOTHERM OF AN IONIC SURACTANT ON A CHARGED SURFACE

In particle flotation, the solid surface adsorbs surfactant ions which, at sufficiently high concentrations, may form a condensed monolayer or hemimicelle. The hydrophobic surface formed by the hemimicelle allows the attachment of bubbles, and flotation occurs. Hemimicelle formation (a two-dimensional phase change) results from van der Waals stabilization of the hydrocarbon tails of adjacent adsorbed surfactant ions. It is affected by the electrical interactions between surfactant ions, electrical interactions between the charged surface sites and the surfactant, and the energy difference between an adsorbed and a free surfactant ion due to chemical bonding.

We use a nonideal Poisson-Boltzmann equation to determine the electric potential in the vicinity of a charged site on the solid surface. This potential is used to calculate the coulombic energy of adsorbed ions interacting with the charged surface and the coulombic repulsion energy developed between adjacent adsorbed surfactant ions. Adsorption isotherms are then calculated by Fowler and Guggenheim's prescription (*21*), taking into account these coulombic forces, the van der Waals attractions

between neighboring adsorbed surfactant ions, and the difference between the chemical potential of an adsorbed surfactant ion and that of an ion in solution.

Analysis

In the calculation of the potential in the vicinity of the plane surface, the charge density is assumed to be discrete, occupying hemispherical sites which are evenly spaced. A form of the Poisson-Boltzmann equation is used which takes into account the finite volumes of the ions (*23*):

$$\frac{1}{r^2}\frac{\partial}{\partial r}\left(r^2\frac{\partial\psi}{\partial r}\right) = \frac{A\sinh\beta'\psi}{1 + B\cosh\beta'\psi} \tag{1}$$

where $\psi(r)$ = electrical potential at a distance r from the center of the charged site

$$A = \frac{8\pi z'ec'_\infty}{(1 - 2c'_\infty/c'_{max})D}$$

$$B = 2c'_\infty/(c'_{max} - 2c'_\infty)$$

D = dielectric constant of water

$z'e$ = |charge| of 1–1 inert electrolyte ions

c'_∞ = concentration in the bulk solution of the 1–1 inert electrolyte establishing the ionic atmosphere

c'_{max} = maximum possible concentration of this electrolyte

Equation (1) is solved numerically using

$$\psi_{n-1} = \psi_n\frac{2r_n}{r_{n-1}} - \psi_{n+1}\frac{r_{n+1}}{r_{n-1}} + \frac{r_n}{r_{n-1}}(\Delta r)^2\frac{A\sinh\beta'\psi_n}{1 + B\cosh\beta'\psi_n} \tag{2}$$

and changing the boundary conditions

$$\psi(\infty) = 0 \tag{3}$$

and

$$\frac{d\psi}{dr}(a) = \frac{-2Q}{a^2D} \tag{4}$$

to

$$\psi(r_N) = 0 \tag{5}$$

and

$$\frac{\psi_2 - \psi_1}{\Delta r} = \frac{-2Q}{a^2D} \tag{6}$$

where a = the radius of an adsorption site

b = the radius of an adsorbed ion
$r_N \simeq 5$ Debye lengths
$= a + (N - 1)\Delta r$
$\psi_n = \psi(r_n)$
Q = charge of central site [$z''e$ for a vacant site, $(z'' + z)e$ for a charged site]
ze = charge of an adsorbed ion
$z''e$ = charge of vacant site

The increase in energy when a surfactant ion is adsorbed on an isolated site on the surface is given by

$$\chi_0 = -[\psi_v(a + b) + x\psi_v(l)]ze + \Delta\mu_0 \tag{7}$$

where $\psi_v(r)$ = the potential at a distance r from a vacant site
$\psi_0(r)$ = the potential at a distance r from an occupied site
l = the distance between adjacent sites
x = the number of nearest neighbor sites
$\Delta\mu_0$ = the difference in chemical potential of an adsorbed ion and that of an ion in solution, $\mu_0^{\text{soln}} - \mu_0^{\text{absorbed}}$

The increase in energy when a pair of nearest neighbors is formed is

$$\frac{2w}{x} = -n(\mathrm{CH_2})c_2 + ze[\psi_0(l) - \psi_v(l)] \tag{8}$$

where $n(\mathrm{CH_2})$ = the number of $\mathrm{CH_2}$ and $\mathrm{CH_3}$ groups in the surfactant hydrocarbon tail
c_2 = the cooperative van der Waals stabilizing energy per $\mathrm{CH_2}$ group

Using these values we can calculate the adsorption isotherms by the method of Fowler and Guggenheim:

$$\sigma = \frac{c}{c'} = \exp\left(\frac{-\chi_0}{kT}\right)\frac{\theta}{1-\theta}\left(\frac{2 - 2\theta}{\beta + 1 - 2\theta}\right)^x \tag{9}$$

$$\beta = \left\{1 - 4\theta(1-\theta)\left[1 - \exp\left(-\frac{2w}{xkT}\right)\right]\right\}^{1/2} \tag{10}$$

$$c' = \left(\frac{2\pi mkT}{h^2}\right)^{3/2} kT\frac{j^S(T)}{j^A(T)} \tag{11}$$

where σ = reduced bulh concentration of surfactant
θ = fraction of sites containing adsorbed surfactant ions
c = concentration of surfactant ion

m = mass of surfactant ion
k = Boltzmann's constant
T = absolute temperature
h = Planck's constant
$j^S(T)$ = partition function for the internal degrees of freedom of a surfactant ion in solution
$j^A(T)$ = partition function for the internal degrees of freedom of an adsorbed surfactant ion

A first approximation for c' can be made by assuming $j^S(T) = j^A(T)$; i.e., the internal rotations and vibrations of an adsorbed ions are the same as those of a free ion. With this assumption and Eq. (11), the value of c' for lauryl sulfate at 25°C is $\simeq 2.85 \times 10^{-7}$ mole/L.

Isotherms have been calculated by estimating c_2 at a distance of 5.1 Å. For adsorption sites with larger spacing, the configuration of adjacent adsorbed molecules is assumed to allow for maximum contact between chains in the hemimicelle at a distance of 5.1 Å. The assumed configuration is shown in Fig. 1. [The cross-sectional area of the hydrocarbon tail is 20.5 Å (*24*). If the area is assumed circular, the radius is 2.55 Å, and therefore the minimum distance between chains is 5.1 Å.] The effective number of CH_2 groups per chain (i.e., the number which interact with adjacent chains) is calculated using 1.43 Å as the vertical distance between carbon atoms. If we use these values there is no van der Waals cooperative stabilizing energy for lauryl sulfate if adsorption sites are more than 16.5 Å apart. This calculation indicates that interaction between non-adjacent hydrocarbon tails is indeed negligible, as assumed.

Below the critical temperature,

$$T_c = \left(\frac{-w}{kx} \log_e\left(\frac{x}{x-2}\right)\right)$$

Two phases are present in equilibrium between the values $\theta_1 < \frac{1}{2}$ and $\theta_2 > \frac{1}{2}$ such the $c(\theta_1) = c(\theta_2) = c(\frac{1}{2})$.

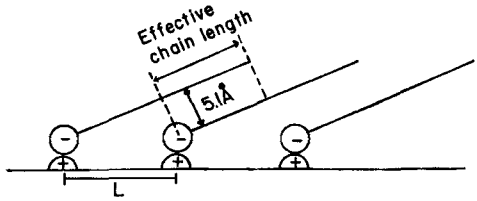

FIG. 1. Configuration of adjacent adsorbed ions adsorbed at lattice sites more than 5.1 Å apart.

RESULTS

Isotherms were calculated with the estimations $c_2 = 2.08 \times 10^{-14}$ erg and $\Delta\mu_0 = 1.0 \times 10^{-13}$ erg. Fuerstenau and Healy found the free energy for the removal of hydrocarbon chains from water to be approximately -0.6 kcal/mole of CH_2 group (*20*) or 4.167×10^{-14} erg/CH_2 group. This value has been reduced by a factor of 2 to avoid counting interactions twice. The radius of the adsorption sites is taken as 2 Å, and the radius of the heads of the adsorbed ions as 3 $Å_0$. Each site is assumed to have six nearest neighbor sites. Isotherms are calculated at 25°C for surfactant ions with a chain length of 12 and a charge of -1.

The effect of the carbon chain length is shown in Fig. 2. With an increase in chain length, the van der Waals stabilizing energy is increased, and a condensed film will form more readily and at lower surfactant concentrations. For chain lengths of less than 11 carbons and adsorption sites 15 Å apart, no van der Waals stabilizing energy is present, and two phases do not form, as shown by Curve 1.

The effect of the charge of the surfactant ion on the isotherm for sites 15 Å apart is shown in Fig. 3. A nonionic molecule is adsorbed (Curve 1) because there is a difference in chemical potential between an adsorbed molecule and a molecule in solution due to chemical binding ($\Delta\mu_0$), but ionic surfactants will adsorb on isolated sites at lower concentrations because of their coulombic attraction for the charged surface. The nonionic molecules form hemimicelles easily because there is no repulsion

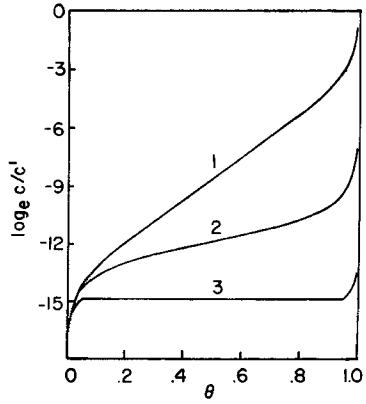

FIG. 2. Effect of hydrocarbon chain length on adsorption isotherms. Model parameters as described in text. Number of carbon atoms in the chain = 6 (1), 12 (2), and 14 (3). In Curve 1 the interaction energy between adjacent sites is positive (repulsive). Sites are 15 Å apart.

between the heads of the molecules and there is a van der Waals attraction between their hydrocarbon tails. Ions of charge -2 (Curve 3) are adsorbed onto an isolated site at lower concentrations than nonionic or -1 ions because of the increased attraction for the charged site. An occupied site creates an effective surface charge of -1; these sites then repel nearby surfactant ions, hindering the formation of hemimicelles.

The effect of temperature is shown in Fig. 4. Lower temperatures allow

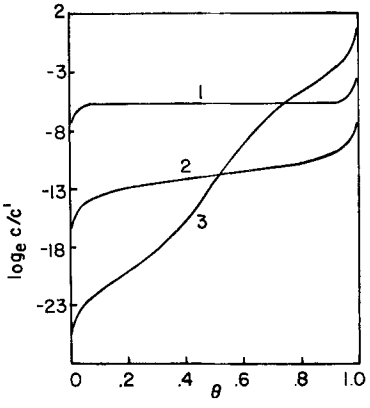

FIG. 3. Effect of surfactant ion charge on adsorption isotherms. Model parameters as given in the text. Charge of the surfactant ion = 0 (1), -1 (2), -2 (3). Sites are 15 Å apart.

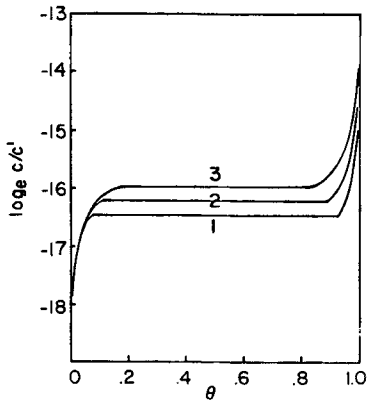

FIG. 4. Effect of temperature on adsorption isotherms. Model parameters as given in the text. Sites are 12 Å apart. Temperature = 15 (1), 25 (2), and 35°C (3).

hemimicelles to form more readily and adsorption to occur at lower concentrations of surfactant since less thermal energy is available for removing adsorbed molecules from the charged surface and for disrupting the attractive forces between adjacent hydrocarbon tails.

Increasing the inert electrolyte concentration (see Fig. 5) tends to shield the surfactant ions from the charged surface, and therefore a higher concentration of surfactant is necessary for adsorption. However, the solutions of higher ionic strength also shield the surfactant ions from each other, reducing the coulombic repulsions between adjacent adsorbed ions and facilitating the formation of condensed films.

In Fig. 6 isotherms are plotted for surface sites of various spacing. For surfactants with a carbon chain length of 12 and adsorption sites spaced

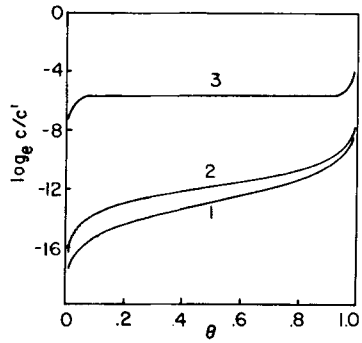

FIG. 5. Effect of inert electrolyte concentration on adsorption isotherms. Sites are 15 Å apart. Inert electrolyte concentration = 1×10^{17} (1), 2×10^{18} (2), and 8×10^{18} ions/cm^3 (3). Other parameters as given in the text.

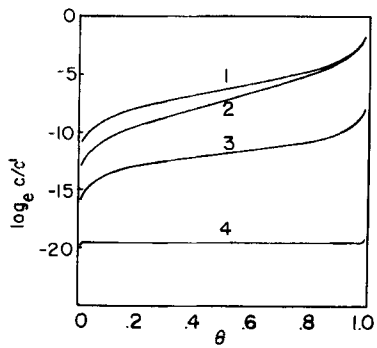

FIG. 6. Effect of distance between sites on adsorption isotherms. L = 50 (1), 25 (2), 15 (3), and 10 Å (4). Other parameters as given in the text.

farther apart than 16.5 Å, no van der Waals stabilizing forces are present, as shown in Curves 1 and 2. The coulombic repulsions between adjacent adsorbed molecules at these distances are increased as the spacing is decreased; therefore the slope of the curve is increased, indicating a lower tendency to form hemimicelles and therefore a lower critical temperature. Because of the increase in effective charge of a surface site (greater charge/unit area) as spacing is decreased, adsorption does occur at lower concentrations than for more widely separated sites. These arguments also apply to Curves 3 and 4 along with the additional factor resulting from the increased effective chain length. Van der Waals forces between adjacent adsorbed ions increase as the distance between the sites is reduced, facilitating the formation of hemimicelles (increasing the critical temperature) and allowing adsorption to occur at lower concentrations. These curves indicate that this increased attraction between adjacent tails has a larger effect on the isotherms than the increased repulsion between adjacent ionic heads as site spacing is reduced.

The effect of the number of nearest neighbor sites is shown in Fig. 7 for a distance between sites which allows for van der Waals attraction between adjacent adsorbed ions. Since the model allows for interactions only between adjacent sites, increasing the number of neighboring sites increases the effective surface charge density although the spacing between sites remains constant. This effect explains the lower concentration of surfactant necessary for adsorption to occur as the number of neighboring sites is increased. The fact that these curves are essentially parallel indicates that the increased coulombic repulsion resulting from more neighboring ions is offset by the increase in the attractive forces between

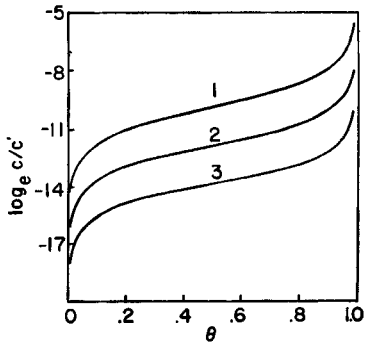

FIG. 7. Effect of number of neighboring sites on adsorption isotherms. L = 15 Å. Other parameters as given in the text. Number of neighboring sites = 4 (1), 6 (2), and 8 (3).

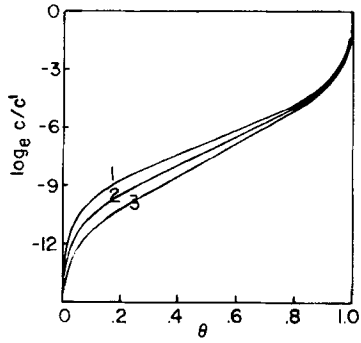

FIG. 8. Effect of number of neighboring sites on adsorption isotherms. L = 25 Å. Number of neighboring sites = 4 (1), 6 (2), and 8 (3); Other parameters as given in the text.

the tails. Figure 8 illustrates the effect of the number of neighboring sites for a distance between sites which does not allow van der Waals attraction between adjacent adsorbed ions. As explained above, increasing the number of neighboring sites lowers the concentration of surfactant necessary for adsorption to occur. The increased coulombic repulsions between neighboring ions inhibit the formation of a more concentrated surface film, as is indicated by the increasing slope of the isotherm as the number of neighboring sites is increased.

We conclude that coulombic interactions between adjacent sites (occupied or unoccupied) may be rather substantial, and can significantly affect the formation of hemimicelles of charged surfactant on solid surfaces.

PARTICLE DETACHMENT

It was previously shown that generally thermal forces are negligible compared to viscous drag forces tending to cause the detachment of floc particles from bubbles in adsorbing colloid and precipitate flotation (*7*, *8*). We recently carried out a rather detailed fluid mechanical calculation of the viscous drag forces on a particle attached to a rising bubble; the results of this work indicated that tangential forces are much larger than radial forces, and suggested the model analyzed below (*22*). In the calculation described here we assume that the size of the floc particles is negligible compared to the size of the bubble. The geometry of the system is shown in Fig. 9. The floc particles are assumed to be confined to a spherical cap on the bottom side of the bubble. We wish to calculate the maximum possible size of this cap, given by θ_0.

The buoyant force acting on the bubble is given by

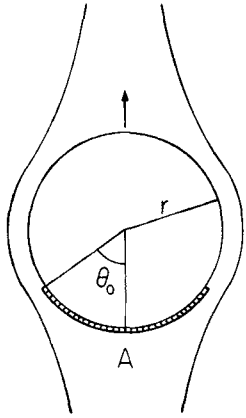

FIG. 9. Model of a spherical cap of floc particles on the bottom of a rising bubble.

$$F_b = {}^4/_3\pi\rho g r^3 \tag{12}$$

where r = bubble radius
g = gravitational acceleration
ρ = density of water

We assume, somewhat roughly, that this is distributed uniformly over the sphere's area, so that the force per unit area is given by

$$f_b = F_b/4\pi r^2 = \rho g r/3 \tag{13}$$

which we take to be the viscous drag per unit area.

The surface (tangential) pressure at θ is then given by

$$P_s = -\int_{\theta_0}^{\theta} \frac{\rho g r}{3} r\, d\theta \tag{14}$$

$$= \rho g r^2(\theta_0 - \theta)$$

$$\leq \frac{\rho g r^2 \theta_0}{3} = P_s^{\max} \tag{15}$$

the surface pressure at the bottom of the cap (at Point A in Fig. 9).

Let ΔG be the work required to detach a particle from the stationary bubble, and α be the area of bubble surface occupied by a particle. Then when

$$\frac{\alpha\rho g r^2 \theta_0}{3} = \Delta G \tag{16}$$

the particle-covered cap on the bottom of the bubble can grow no more, since the surface pressure would expel the particles out of the film at A. Then

$$\begin{aligned} \theta_0 &= \frac{3\Delta G}{\alpha\rho g r^2}, \qquad \theta_0 < \pi \\ &= \pi, \qquad \text{if } \frac{3\Delta G}{\alpha\rho g r^2} > \pi \end{aligned} \tag{17}$$

The surface area of the particle-covered cap is then given by

$$\begin{aligned} S_c &= \int_0^{\theta_0}\int_0^{2\pi} r^2 \sin\theta \, d\phi \, d\theta = 2\pi r^2(1 - \cos\theta_0) \\ &= 4\pi r^2, \qquad r \leq \left(\frac{3\Delta G}{\pi\alpha\rho g}\right)^{1/2} \\ &= 2\pi r^2\left(1 - \cos\frac{3\Delta G}{\alpha\rho g r^2}\right), \qquad r > \left(\frac{3G}{\alpha\rho g\pi}\right)^{1/2} \end{aligned} \tag{18}$$

For $r \gg (3\Delta G/\pi\alpha\rho g)^{1/2}$ we have

$$S_c \cong 2\pi r^2\left[1 - 1 + \frac{1}{2!}\left(\frac{3\Delta G}{\alpha\rho g r^2}\right)^2 - \cdots\right]$$

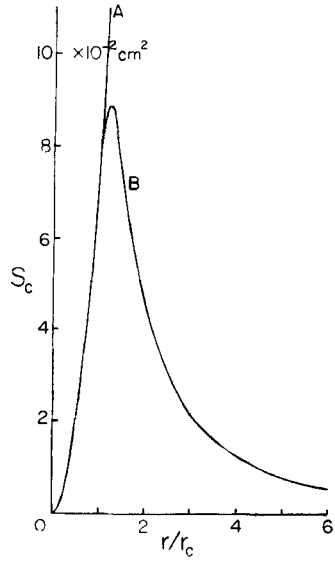

FIG. 10. Plot of cap area, S_c (Curve B), against reduced bubble radius, r/r_c. $r_c = 0.079$ cm. Curve A gives total bubble area of a bubble of radius r.

$$S_c = 9\pi\left(\frac{\Delta G}{\alpha\rho g}\right)^2 \frac{1}{r^2} \tag{19}$$

which approaches zero as r increases.

For $\alpha = \pi a^2$, $a = 10^{-5}$ cm (particle radius), $\Delta G \cong 2 \times 10^{-9}$ erg (7), we find that the maximum radius of a bubble which can be completely covered is given by

$$r_c = \left(\frac{3\Delta G}{\pi\alpha\rho g}\right)^{1/2} = 0.079 \text{ cm} \tag{20}$$

$\theta_0 = \pi/2$ when $r^2 = 2r_c^2$, so that bubbles of radius 0.112 cm will have at most 50% coverage.

We note that improving this calculation by making a more accurate calculation of surface tangential pressure as a function of θ will require calculations of fluid flow patterns around the bubble which are far from the Stokes' law regime. The rise velocity for a bubble or radius 0.1 cm (calculated by Oseen's improvement to Stokes' law) is 7.5 cm/sec. This

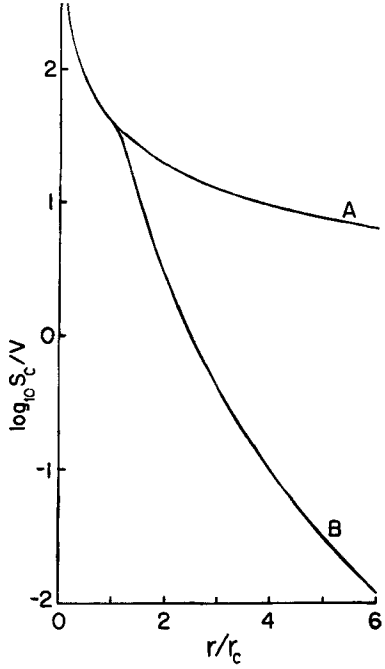

FIG. 11. Plot of $\log_{10} S_c/V$ against reduced bubble radius (Curve B). $r_c = 0.079$ cm. Curve A gives surface to volume ratio of a spherical bubble of radius r.

yields a Reynolds number of 150, which means that one is well out of the domain of creeping flow.

Figure 10 shows a plot of cap surface area versus r/r_c for the floc parameters listed above. The curve labeled A gives the total surface area of the bubble; that labeled B, the area of the cap. The area per bubble which can be coated with floc particles S_c evidently decreases quite rapidly as the bubble radius increases above about $1.2r_c$, indicating that air pumped into a flotation cell in the form of bubbles of radius much in excess of this value is air wasted. In Fig. 11 we plot $\log_{10} S_c/V$, where V is the bubble volume; we see a very rapid drop-off in this quantity as r exceeds r_c. This plot indicates that air bubbles of the smallest size are the most efficient; we must, however, note that the rise velocity of a bubble in the Stokes' law regime is given by

$$v = 2\rho g r^2/9\eta \tag{21}$$

so that the air flow rate which can be handled by a given flotation cell must decrease quite drastically with decreasing r if r is sufficiently small.

DIFFERENTIAL CAPACITANCE OF A DOUBLE LAYER

In a number of previous calculations on adsorbing colloid flotation and precipitate coagulation (*5–12*, *23*), we used a Poisson-Boltzmann equation which was modified to take into account the finite volumes of the ions in the diffuse double layer in the vicinity of a plane surface. If one uses a linearized Poisson-Boltzmann equation

$$d\psi/dx^2 = \kappa^2\psi \tag{22}$$

one obtains, on using the electrical neutrality requirement,

$$\sigma = \frac{\kappa D}{4\pi}\psi_0 \tag{23}$$

where $\kappa^2 = 8\pi z^2 e^2 c_\infty/DkT$
ψ = electric potential
$|ze|$ = charge on ions of 1–1 electrolyte
D = dielectric constant of water
c_∞ = bulk salt concentration, cations/cm^3
k = Boltzmann's constant
T = absolute temperature
σ = surface charge density

The differential capacitance of the double layer for this model is then given

by a constant, independent of ψ_0,

$$C_D = \frac{d\rho}{d\psi_0} = \frac{\kappa D}{4\pi} \tag{24}$$

in marked disagreement with experiment (*25*).

With a nonlinearized Poisson-Boltzmann equation in which the finite volumes of the electrolyte ions are neglected, one runs into similar difficulties (*25*). The equation is

$$\frac{d^2\psi}{dx^2} = \frac{8\pi e c_\infty}{D} \sinh\left(\frac{ze\psi}{kT}\right) \tag{25}$$

and the resulting differential capacitance is (*25*)

$$C_D = \frac{\kappa D}{4\pi} \cosh\frac{ze\psi_0}{kT} \tag{26}$$

In fact, for small $|\psi_0|$ the differential capacitance does appear to have a hyperbolic cosine dependence on ψ_0, but for larger $|\psi_0|$ Eq. (26) predicts values of C_D which are far too large; a typical experimental curve is sketched in Fig. 12. Such curves are commonly obtained by partitioning the double layer into a Stern layer, in which monolayer absorption of ions of finite size takes place, and an outer, diffuse layer (Gouy layer).

Actually, by using a Poisson-Boltzmann equation which takes into account the finite volumes of the ions, it appears to be possible to obtain differential capacitance curves of the type shown in Fig. 12 within a single,

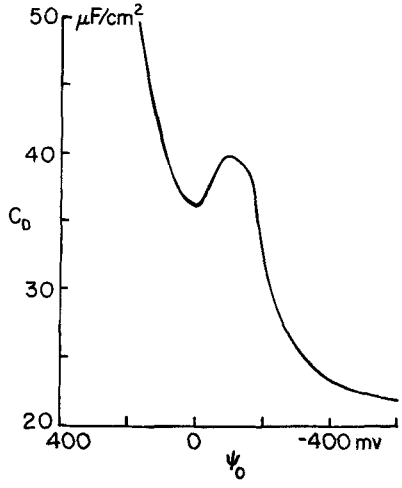

FIG. 12. Representative plot of differential capacitance C_D vs surface potential ψ_0.

unified treatment. We use a Poisson-Boltzmann equation derived earlier (*23*),

$$\frac{d^2\psi}{dx^2} = \frac{A \sinh (ze\psi/kT)}{1 + B \cosh (ze\psi/kT)} \tag{27}$$

where $A = \dfrac{8\pi zec_\infty}{(1 - 2c_\infty/c_{max})D}$

$B = 2c_\infty/(c_{max} - 2c_\infty)$

$c_{max} = 1/\bar{v}$

$\bar{v}$ = volume of a hydrated anion if $\psi \geq 0$

= volume of a hydrated cation if $\psi < 0$

A first integral to this equation which satisfies the boundary conditions $d\psi/dx \to 0$ as $x \to \infty$ is

$$\frac{d\psi}{dx} = -\frac{\psi_0}{|\psi_0|}\left[\frac{2AkT}{zeB} \log_e \frac{1 + B \cosh (ze\psi/kT)}{1 + B}\right]^{1/2} \tag{28}$$

The surface charge density is then given by the electrical neutrality requirement as

$$\sigma = -\frac{D}{4\pi}\frac{d\psi(0)}{dx} \tag{29}$$

which yields

$$\sigma = \frac{\psi_0}{|\psi_0|}\frac{D}{4\pi}\left[\frac{2AkT}{zeB} \log_e \frac{1 + B \cosh (ze\psi_0/kT)}{1 + B}\right]^{1/2} \tag{30}$$

The differential capacitance of the double layer, $C_D = d\sigma/d\psi_0$, is given by

$$C_D = \frac{D}{4\pi}\left(\frac{AzeB}{2kT}\right)^{1/2}\left[\log \frac{1 + B \cosh (ze\psi_0/kT)}{1 + B}\right]^{-1/2} \times \frac{|\sinh (ze\psi_0/kT|}{1 + B \cosh (ze\psi_0/kT)} \tag{31}$$

Figure 13 shows the effects of ionic strength on plots of differential capacitance versus surface potential. We have more or less arbitrarily chosen the molar volume of the anion to be 50.0 cm^3/mole, and that of the cation to be 100.0 cm^3/mole. We note that these curves exhibit a minimum in C_D at $\psi_0 = 0$, that they show the humps commonly found near zero surface potential, and that C_D decreases, leveling out to a slowly varying value as $|\psi_0|$ increases. The shape and position of the hump on the left side can be varied by changing the molar volume of the cation; the hump on the right can be similarly varied by changing the molar volume of the anion. The extent of the effects of ionic molar volume is indicated by a comparison of Fig. 13 with Fig. 14, for which the molar volumes are

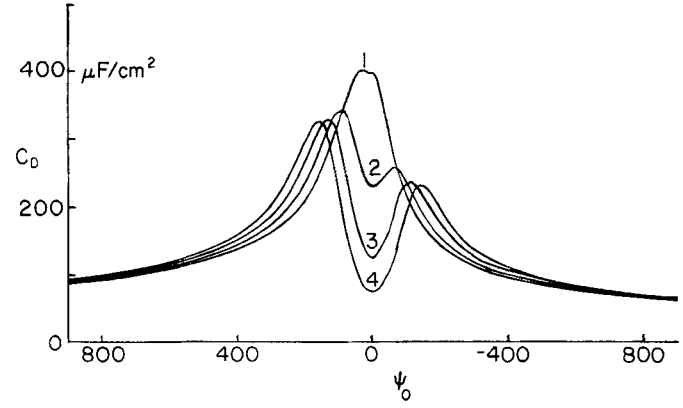

FIG. 13. Plots of C_D vs ψ_0 (mV) at various ionic strengths. $\bar{v}$ (anions) = 50 cm³/mole; $\bar{v}$ (cations) = 100 cm³/mole; T = 298°K; z = 1; salt concentration = 3.0, 1.0, 0.3, and 0.1 mole/L for Curves 1 through 4, respectively.

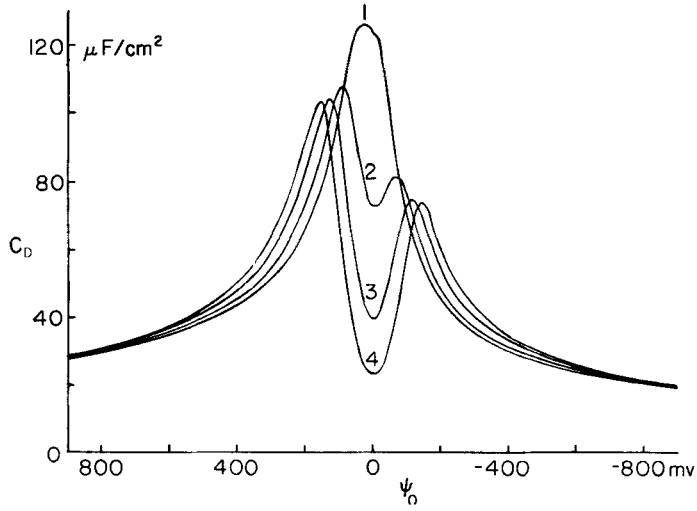

FIG. 14. Plots of C_D vs ψ_0 at various ionic strengths. $\bar{v}$ (anions) = 500 cm³/mole; $\bar{v}$ (cations) = 1000 cm³/mole; T = 298°K; z = 1; salt concentration = 0.3, 0.1, 0.03, and 0.01 mole/L for Curves 1 through 4, respectively.

500 cm³/mole (anion) and 1000 cm³/mole (cation). Increasing the molar volumes markedly decreases C_D, as one would expect.

Acknowledgment

This work was supported by a grant from the Vanderbilt University Research Council.

REFERENCES

1. R. Lemlich (ed.), *Adsorptive Bubble Separation Techniques*, Academic, New York, 1972.
2. P. Somasundaran, *Sep. Sci.*, *10*, 93 (1975).
3. R. B. Grieves, *Chem. Eng. J.*, *9*, 93 (1975).
4. A. N. Clarke and D. J. Wilson, *Sep. Purif. Methods*, *7*, 55 (1978).
5. D. J. Wilson, *Sep. Sci.*, *12*, 231 (1977).
6. D. J. Wilson, *Ibid.*, *12*, 447 (1977).
7. D. J. Wilson, *Sep. Sci. Technol.*, *13*, 107 (1978).
8. B. L. Currin, F. J. Potter, D. J. Wilson, and R. H. French, *Ibid.*, *13*, 285 (1978).
9. A. N. Clarke, D. J. Wilson, and J. H. Clarke, *Ibid.*, *13*, 573 (1978).
10. D. J. Wilson and R. M. Kennedy, *Ibid.*, *14*, 319 (1979).
11. B. L. Currin, R. M. Kennedy, A. N. Clarke, and D. J. Wilson, *Ibid.*, *14*, 669 (1979).
12. J. C. Barnes, J. M. Brown, N. A.-K. Mumallah, and D. J. Wilson, *Ibid.*, *14*, 777 (1979).
13. A. M. Gaudin and D. W. Fuerstenau, *Trans. AIME*, *202*, 958 (1955).
14. D. W. Fuerstenau, T. W. Healy, and P. Somasundaran, *Ibid.*, *229*, 321 (1964).
15. P. Somasundaran, T. W. Healy, and D. W. Fuerstenau, *J. Phys. Chem.*, *68*, 3562 (1964).
16. P. Somasundaran and D. W. Fuerstenau, *Ibid.*, *70*, 90 (1966).
17. T. Wakamatsu and D. W. Fuerstenau, *Adv. Chem. Ser.*, *79*, 161 (1978).
18. P. Somasundaran, *Trans. AIME*, *241*, 105 (1968).
19. P. Somasundaran and D. W. Fuerstenau, *Ibid.*, *241*, 102 (1968).
20. D. W. Fuerstenau and T. W. Healy, in Ref. *1*, p. 91.
21. R. Fowler and E. A. Guggenheim, *Statistical Thermodynamics*, Cambridge University Press, 1952, pp. 429–443.
22. R. H. French and D. J. Wilson, *Sep. Sci. Technol.*, In Press.
23. D. J. Wilson, *Sep. Sci.*, *11*, 391 (1976).
24. N. K. Adam, *The Physics and Chemistry of Surfaces*, Dover Publications, New York, 1968.
25. J. O'M. Bockris and A. K. N. Reddy, *Modern Electrochemistry*, Vol. 2, Plenum, New York, 1970, pp. 724–733, 753–762.

Received by editor August 9, 1979